J. Biochem. 2009;146(2)219–229
doi:10.1093/jb/mvp061

The peptidoglycan-binding (PGB) Domain of the *Escherichia coli* Pal Protein can also Function as the PGB Domain in *E. coli* Flagellar Motor Protein MotB

Yohei Hizukuri, John Frederick Morton, Toshiharu Yakushi*, Seiji Kojima and Michio Homma†

Division of Biological Science, Graduate School of Science, Nagoya University, Furo-Cho, Chikusa-Ku, Nagoya 464-8602, Japan

Received December 22, 2008; accepted March 25, 2009; published online April 13, 2009

The bacterial flagellar stator proteins, MotA and MotB, form a complex and are thought to be anchored to the peptidoglycan by the C-terminal conserved peptidoglycan-binding (PGB) motif of MotB. To clarify the role of the C-terminal region, we performed systematic cysteine mutagenesis and constructed a chimeric MotB protein which was replaced with the peptidoglycan-associated lipoprotein Pal. Although this chimera could not restore motility to a *motB* strain, we were able to isolate two motile revertants. One was F172V in the Pal region and the other was P159L in the MotB region. Furthermore, we attempted to map the MotB Cys mutations in the crystal structure of *Escherichia coli* Pal. We found that the MotB mutations that affected motility nearly overlapped with the predicted PG-binding residues of Pal. Our results indicate that, although the functions of MotB and Pal are very different, the PGB region of Pal is interchangeable with the PGB region of MotB.

Key words: bacterial flagella, *Escherichia coli*, MotB, peptidoglycan-binding protein, Pal.

Abbreviations: PG, peptidoglycan; PGB, peptidoglycan-binding; TCA, trichloric acid.

Many bacteria swim using organelles called flagella, which rotate and function like a screw. The flagellum is composed of at least three parts: a helical filament extending from the cell body, a motor embedded in the cytoplasmic membrane that drives the rotation of the filament, and a flexible hook that connects the filament and the motor (*1*). In *Escherichia coli* and *Salmonella enterica* serovar Typhimurium, genetic, biochemical and biophysical research has been actively carried out to reveal the mechanism of rotation of the flagellar motor. In these organisms, the driving force for rotation of the flagellar motor is generated by converting the electrochemical proton potential into mechanical force. This energy conversion is thought to be conducted by the electrostatic interaction between the rotor protein FliG and the stator protein MotA (*2*). The rotor protein FliG, together with FliM and FliN, form the C ring, which lies on the cytoplasmic side of the membrane-embedded basal body (*3*). On the other hand, MotA forms the stator complex with MotB, and this complex is thought to function as a proton channel in the inner membrane (*4–7*). MotA has four transmembrane regions and a large cytoplasmic loop region (*8*), whereas MotB has a single N-terminal transmembrane region and a large C-terminal periplasmic region, which is believed to associate with the peptidoglycan (PG) layer (*9*, *10*). For the stator complex, four MotA and two MotB proteins assemble to form a proton channel (*11–14*). The stator complex is believed to be anchored to the PG layer around the flagellar basal body by the C-terminal region of MotB. The Asp^{32} residue in the single transmembrane helix of *E. coli* MotB is highly conserved among flagellated bacteria and is critical for motor function. This Asp residue is believed to function as a proton-binding site in the stator complex (*15*). A conformational change in the stator coupled with the proton flow is thought to generate the driving force for motor rotation (*16*).

The C-terminal region of MotB has a consensus PGB motif (*10*, *17*). Recently, a crystal structure of the C-terminal region of MotB from *Helicobacter pylori* was reported (*18*). The PGB motif is widespread in many outer membrane proteins, such as OmpA and Pal, and other proteins in Gram-negative bacteria. Crystal or NMR structures of several proteins containing a PGB motif have been solved, *e.g.* peptidoglycan-associated lipoprotein Pal from *E. coli* (PDB accession code, 1oap) and *Haemophilus influenzae* (*19*), the putative outer membrane protein RmpM from *Neisseria meningitidis* (*20*), and the *Vibrio*-specific flagellar T ring protein MotY from *Vibrio alginolyticus* (*21*). In the *H. influenzae* Pal, the NMR structure of the complex between the C-terminal PGB region of Pal and the biosynthetic

*Present address: Applied Molecular Bioscience, Graduate School of Medicine, Yamaguchi University, Yamaguchi 753-8515, Japan.
†To whom correspondence should be addressed.
Tel: +81-52-789-2991, Fax: +81-52-789-3001,
E-mail: g44416a@cc.nagoya-u.ac.jp

peptidoglycan-precursor (PG-P), UDP-*N*-acetylmuramyl-L-Ara-α-D-Glu-*m*-Dap-D-Ala-D-Ala has been reported (*19*). The authors reported that the PG-P binding site is located at a surface cavity in the Pal structure formed by the β1-α2 and β2-α3 loop regions, and they speculate that this binding between Pal and PG-P may be conserved in other PGB proteins in Gram-negative bacteria (*19*). The 3D structures of the PGB regions of MotY, Pal of *E. coli* and RmpM as well as *H. pylori* MotB show remarkable structural similarity (*18*, *21*) although the sequence homologies among them are very limited. From these insights, the PGB region of *E. coli* MotB is also expected to have a structure similar to other PGB proteins and to associate with the PG layer in a similar manner.

Pal is a universal outer membrane protein and one of the best-studied PGB proteins in Gram-negative bacteria. Pal is secreted by its N-terminal signal sequence across the cytoplasmic membrane, and it is transported to the outer membrane by the LolABCDE system after cleavage of the signal sequence (*22–25*). Pal is anchored to the outer membrane by its N-terminal *N*-diacyl glyceride moiety (*26*), and it interacts strongly with the PG layer by its C-terminal PGB region (*26–29*). Pal belongs to the Tol-Pal system, which is highly conserved among Gram-negative bacteria and thought to have a role in the maintenance of cell envelope integrity (*30*). The Tol-Pal system is mainly composed of five proteins: TolA, TolB, TolQ, TolR and Pal. TolA is anchored to the cytoplasmic membrane by its N-terminal transmembrane helix, and the C-terminal region of TolA extends into the periplasmic space and interacts with the periplasmic protein TolB and the outer membrane-anchored Pal (*31–33*). The three-transmembrane protein TolQ and the single-transmembrane protein TolR interact with TolA by their transmembrane helices. Thus, the Tol-Pal system is thought to form a *trans*-envelope bridge linking the inner and outer membranes to the PG layer. TolQ and TolR have been proposed to form a proton or ion channel that converts proton motive force (pmf) to mechanical energy to allow the Tol-Pal system to function (*34*, *35*). There are structural and functional homologies between the Tol-Pal system and the Exb-TonB system, which is involved in iron siderophore and cobalamin uptake across the outer membrane (*36*). It has been pointed out that TolQ-TolR and ExbB-ExbD proteins have weak sequence homologies with the MotA-MotB proteins and that these three systems function as ion potential-driven molecular motors (*16*, *34*). For example, the important ion binding residue Asp^{32} in *E. coli* MotB is conserved in both TolR (Asp^{23}) and ExbD (Asp^{25}) (*34*).

Biochemical and structural research on the PGB region of MotB is less advanced than that of Pal. In this study, to obtain new insight into the PGB region of MotB, we analysed Cys-mutagenized *E. coli* MotB variants and a MotB chimeric protein in which the PGB region was replaced with that from *E. coli* Pal. The chimeric protein was non-functional in its original form; however, we could isolate two motile revertants of the MotB-Pal chimera that complement the *motB* mutant to some degree. This means that the PGB region of MotB can be replaced by the PGB region of Pal. We also discuss the functionally important residues identified by our mutagenic analysis in the context of the crystal structure of *E. coli* Pal.

MATERIALS AND METHODS

Bacterial Strains, Growth Conditions and Media—The *E. coli* strains used in this work are listed in Table 1. The Δ*tolB-pal* strain JC7752 was kindly supplied by Hélène Bénédetti (CBM, CNRS) and Shin-ichiro Narita (University of Tokyo). *Escherichia coli* cells were cultured at 37°C or at 30°C in LB medium (1% Bacto tryptone, 0.5% yeast extract and 0.5% NaCl) or in TG medium [1% Bacto tryptone, 0.5% NaCl and 0.5% (w/v) glycerol]. When necessary, ampicillin and kanamycin were added to a final concentration of 50 μg/ml.

Construction of Plasmids—Routine DNA manipulations were carried out according to standard procedures (*37*). The plasmids used in this work are listed in Table 1. To construct pYZ501, the *pal* gene was PCR amplified from *E. coli* W3110 chromosomal DNA and *Eco*RI and *Hin*dIII restriction enzyme sites were added upstream of the promoter and downstream of the stop codon. The 0.6 kb *Eco*RI/*Hin*dIII fragment was inserted into the pBAD24 vector to obtain pYZ501.

Chimeric MotB protein expressing plasmids were constructed by a two-step PCR method. To obtain the chimeric *motB-pal* gene, two fragments were PCR amplified using two sets of primers: (i) Using the upstream primer and MotB-Pal(−) (5′-CTTGTCCAGATCGAACATCGGGCGATTCTGGCTATC-3′; nucleotides corresponding to *motB* are underlined for all primers described below) and the pJN726 plasmid carrying the *E. coli motAB* operon (*38*) as the template, the *motA* gene and the *motB*-part of the chimeric gene, adding an *Xba*I site upstream of the promoter of the *motAB* operon were amplified; (ii) using MotB-Pal(+) (5′-GCCAGAATCGCCCGATGTTCGATCTGGACAAGTACG-3′) and the downstream primer and pYZ501 carrying the *pal* gene as the template, the *pal*-part of the chimeric gene was amplified. Next, these two fragments were mixed and PCR amplified to obtain a full-length *motA/motB-pal* sequence. Amplified fragments were digested with *Xba*I and *Hin*dIII, and the 1.7 kb fragment was inserted into the pBAD24 vector to obtain pJFM10.

Table 1. ***Escherichia coli* strains and plasmids.**

Strain or plasmid	Genotype or description[a]	Reference or source
Strains		
RP437	F⁻ *thi thr leu his met eda rpsL* wild-type for chemotaxis	(*56*)
YZ12-1	RP437 Δ*flgI* Δ*motAB*::*cat*	(*38*)
RP6894	Δ*motAB*	(*44*)
JC7752	1292 Δ*tolB-pal*	(*57*)
Plasmids		
pBAD24	P_{BAD} *araC* Amp^r	(*58*)
pYZ301	pSU38 *Ec flgI*, Km^r	(*38*)
pJN726	pBAD24 *Ec motAB*	(*38*)
pYZ501	pBAD24 *Ec pal*	This work
pJFM10	pBAD24 [*Ec* MotA/MotB-Pal]	This work

[a]Amp^r, ampicillin resistant; Km^r, kanamycin resistant; P_{BAD}, *araBAD* promoter.

To construct Cys-substituted MotB variants and residue substitutions at Phe^{172} of MotB-Pal and Phe^{63} of Pal, site-directed mutagenesis was performed as described previously (*38*).

Detection of Proteins—For immunoblotting, anti-*E. coli* MotA and anti-*E. coli* MotB antibodies, called MotA266 and MotB2, respectively, were raised against synthetic peptides (NH2-GCSERPSFIELEEHVRAVKN-OH for MotA266 and NH2-KNQAHPIIVVKRRKAKSHGC-OH for MotB2) corresponding to partial sequences of *E. coli* MotA (MotA Ser^{268} to Asn^{285}) and MotB (MotB Lys^{2} to Gly^{20}), and IgG fractions were affinity-purified (Biologica Co.). The anti-*E. coli* Pal antibody (*24*) was a generous gift from Hajime Tokuda (University of Tokyo) and was originally prepared by Takeshi Mizuno (Nagoya University).

Disulfide Cross-linking—In vivo disulfide cross-linking in the presence of Cu(II)(*1,10*-phenanthroline)$_3$ (referred to as Cu-phenanthroline in this article) was performed using a previously described method (*39*) with slight modifications. Sixty millimolar Cu-phenanthroline solution {60 mM Cu(II)SO_4-5H_2O, 200 mM *1,10*-phenanthroline monohydrate (nakalai tesque), 50 mM $NaHPO_4$ (pH7.8)} was stored at −20°C in the dark. Cells in exponential growth phase (OD_{660} = 1.0) from 1 ml in TG medium containing 50 μg/ml ampicillin and kanamycin and 0.04% L-arabinose at 30°C were harvested by centrifugation, and suspended in 1 ml of Wash Buffer (10 mM potassium phosphate buffer, pH 7.0, containing 0.1 mM EDTA-K). Cells were divided into two aliquots, then centrifuged and resuspended in 200 μl of MLM Buffer (Wash Buffer containing 10 mM DL-lactate/KOH and 0.1 mM L-methionine) with or without 1 mM Cu-phenanthroline. Each sample was incubated at room temperature for 30 min. in the dark. To stop the reaction, 40 μl of 6× Stop solution (210 mM Tris–HCl, pH 7.0, 15 mM EDTA–Na, pH 7.0, 15 mM *N*-ethylmaleimide) was added. Each sample was centrifuged again, resuspended in 50 μl of SDS loading buffer without β-mercaptoethanol, and boiled at 100°C for 5 min. Samples were separated by SDS–PAGE and analyzed by immunoblotting.

Motility Assays—Swarming ability was assayed as follows. A 2 μl of overnight cultures (grown on LB medium at 37°C) were dropped on a soft agar T broth plate (1% Bacto tryptone, 0.5% NaCl and 0.27% Bacto agar) containing 50 μg/ml ampicillin and/or kanamycin. To induce protein production, 0.04% L-arabinose was included in the plate. The plates were incubated at 30°C. Relative swarm sizes of the MotB Cys mutants were calculated by normalizing to the diameter of the swarm ring of the wild-type MotB-expressing cells after subtracting the diameter of the swarm ring of the vector-containing cells.

Cysteine Modification by Methoxypolyethylene Glycol 5,000 Maleimide (mPEG-maleimide)—Cysteine modification using the thiol-specific reagent mPEG-maleimide was described previously (*38*). Briefly, cells at exponential growth phase in TG medium containing 50 μg/ml ampicillin and kanamycin and 0.04% L-arabinose were harvested by centrifugation, then suspended in 1 ml of Wash Buffer. The cells were centrifuged again and resuspended in 25 μl of MLM Buffer. A 25 μl aliquot of mPEG-maleimide reaction buffer (MLM Buffer containing 4 mM mPEG-maleimide) was added to cell suspensions and mixed well, then incubated with shaking at 37°C for 30 min. To terminate the reaction, 5 μl of β-mercaptoethanol was added, followed by 5 μl of 10% SDS. The sample solution was boiled at 100°C for 5 min and mixed with 15 μl of 5× SDS loading buffer containing β-mercaptoethanol. MotB proteins were separated by SDS–PAGE and analyzed by immunoblotting. mPEG-maleimide labeling efficiency was obtained by dividing the intensity of the ~5 kDa shifted band by the total band intensity of MotB.

Peptidoglycan-binding Assay—Purification of PGB proteins was performed by the method described previously (*33*) with slight modifications. An overnight culture (grown on LB medium at 30°C) was inoculated at a 100-fold dilution into LB medium containing 50 μg/ml ampicillin and 0.004% L-arabinose and cultured at 30°C. At the exponential growth phase, 300 μl of cultured cells (OD_{660} = 1.0) were harvested by centrifugation. The cells were suspended in 900 μl of SDS-Extraction Buffer [100 mM Tris–HCl, pH 8.0, 100 mM NaCl, 10% (v/v) glycerol, 2% (w/v) SDS, room temperature] and transferred into a test tube. The cells were incubated in a water bath at 37°C for 1 h with shaking, then centrifuged at 130,000*g* for 1 h at 25°C and divided into soluble and insoluble fractions. Insoluble materials (*i.e.* PG-binding fractions) were washed with 900 μl of SDS-Extraction Buffer, sonicated for 30 s at room temperature, then boiled at 100°C for 15 min. The soluble and insoluble fractions (300 μl each) were collected by TCA precipitation without cooling, then suspended in 100 μl of SDS loading buffer with β-mercaptoethanol, and boiled at 100°C for 5 min. Five μl of SDS samples were used for SDS–PAGE and immunoblot analysis.

RESULTS

Systematic Cys Mutagenesis of the MotB C-terminus—The C-terminal region of MotB has a PGB motif, and MotB is believed to be anchored to the PG layer by this motif (*10*, *17*). Deletion analysis of the C-terminal region of PomB (*40*), which is a *Vibrio* homolog of MotB, and fluorescent observation of the GFP-fused C-terminal-truncated PomB (*41*) have revealed that the C-terminal PGB region is essential for assembly of the stator complex around the flagellar rotor. When we started this project there was very little structural information on the C-terminal PGB region of MotB, so we performed a systematic cysteine mutagenesis analysis on the C-terminus of *E. coli* MotB to investigate the role of the PGB region and to obtain structural insights. We previously constructed a strain that contains two plasmids, pYZ301 carrying the *E. coli flgI* gene and pJN726 carrying the *E. coli motAB* operon in the *E. coli* strain YZ12-1 (Δ*flgI* Δ*motAB*::*cat*) to investigate the flagellar P-ring protein FlgI (*38*). This strain had almost the same motility phenotype as a wild-type strain, so we used this strain for the Cys mutagenesis experiments on MotB.

We constructed a series of systematically-Cys-substituted MotB variants. Every tenth residue in the

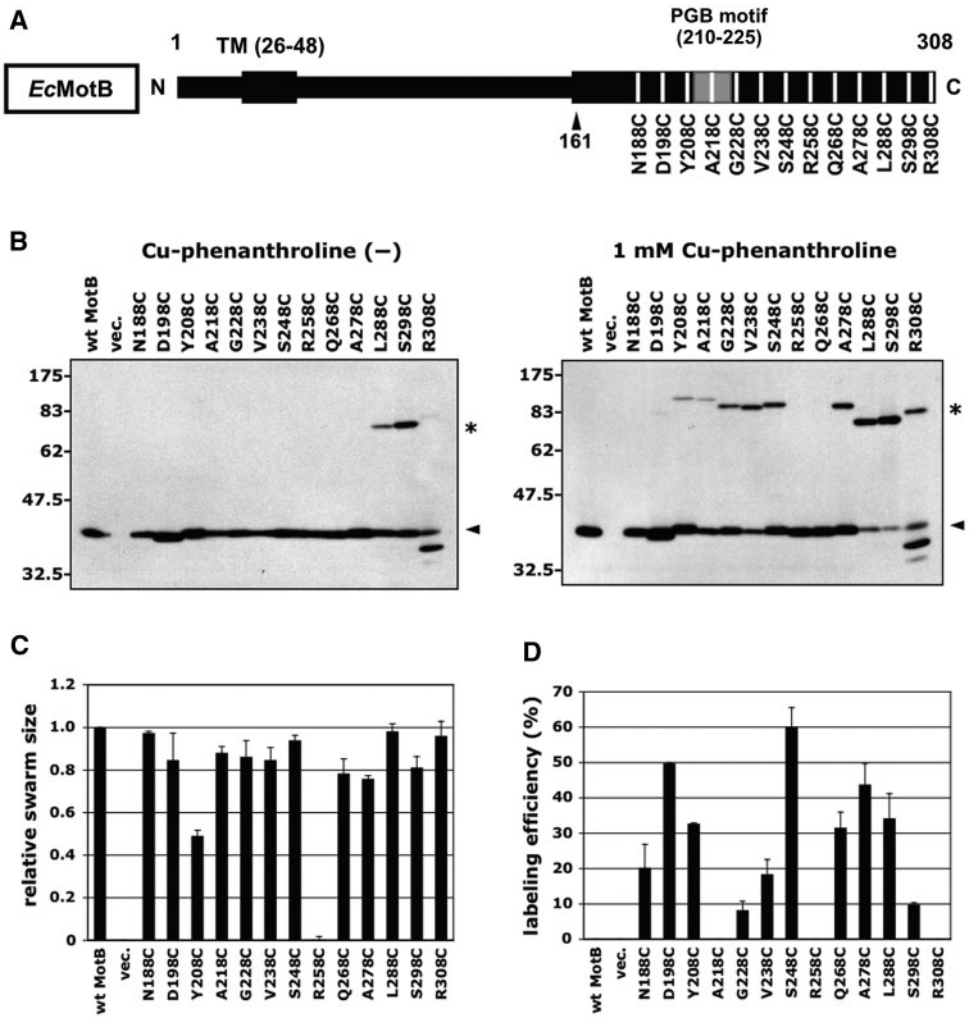

Fig. 1. **Characterization of systematically substituted MotB Cys mutants.** (A) Primary structure of *E. coli* MotB. TM indicates the transmembrane region. PGB motif shows the peptidoglycan binding motif (N..L...RA..V...L) proposed by Koebnik (*17*); that sequence is $\underline{N}^{210}WE\underline{L}SAD\underline{RA}NA\underline{S}RRE\underline{L}^{225}$ in *E. coli* MotB. The white vertical bands indicate the residues substituted with Cys in this study. Phe^{161} is the junction site of the chimeric MotB protein constructed in this work. (B) *In vivo* disulfide cross-linking of the systematically substituted MotB Cys variants by the oxidant Cu-phenanthroline. The MotB proteins from YZ12-1 (Δ*flgI* Δ*motAB*::*cat*) cells harboring pYZ301 (FlgI) and pJN726 (wt MotA/MotB), pBAD24 (vector) or pJN726 derivatives containing a series of MotB Cys variants were detected by immunoblotting using anti-MotB antibodies. Protein expression was induced with 0.04% L-arabinose. Cells were harvested, washed and incubated with (*right panel*) or without (*left panel*) 1 mM Cu-phenanthroline at room temperature for 30 min. The arrowheads on the right side indicate monomeric MotB (34 kDa), while the asterisk indicates the predicted cross-linked dimer. (C) Motility of the MotB Cys variant expressing cells. Relative swarm sizes of the MotB Cys mutants are indicated. A drop (2 μl) of overnight culture was inoculated on 0.27% soft-agar T broth plates and incubated at 30°C. The swarm assays were repeated three times independently and the relative swarm sizes determined in each experiment were averaged. (D) Cysteine modification of the MotB Cys variants by mPEG-maleimide. For the mPEG-maleimide modification, cells were harvested, washed and incubated with 2 mM mPEG-maleimide at 37°C for 30 min. Modified MotB proteins were analysed by SDS–PAGE and immunoblotting using anti-MotB antibodies. mPEG-maleimide labeling efficiency was obtained by dividing the intensity of the shifted band into the total band intensity of MotB.

MotB protein from the C-terminus (Arg^{308}) was substituted with Cys (Fig. 1A). MotB has the PGB motif (N..L...RA..V...L) proposed by Koebnik (*17*) at Asn^{210}-Leu^{225}. To cover this PGB motif, we constructed 13 MotB Cys variants from N188C to R308C. We examined the amounts of the MotB Cys mutant proteins by immunoblotting using anti-MotB antibodies. Most of the mutant proteins did not decrease in amount compared to the wild-type MotB (data not shown, almost the same as the left panel in Fig. 1B). For MotB R308C, additional bands, which are probably degradation products, were detected at sizes smaller than MotB (34 kDa). In the absence of the reductant β-mercaptoethanol, proteins larger than MotB, which are probably disulphide cross-linked products, were detected for MotB L288C, S298C and R308C (data not shown, almost same as the left panel in Fig. 1B). These cross-linked products seemed to be homodimers of MotB as judged by comparison with the size reported in the MotB cross-linking experiment (*42*). Dimer formation by these three variants was

enhanced by treatment with the oxidant Cu-phenanthroline (Fig. 1B, the right panel). Most of the variants formed putative dimers when treated with Cu-phenanthroline.

To assess the effects of the Cys substitutions in MotB on its function, we examined the swarming ability of cells expressing the MotB Cys variants (Fig. 1C). We measured the sizes of the swarm ring after incubation of the cells on a 0.27% soft agar plate, and calculated the relative swarm sizes for each MotB Cys mutant against wild-type MotB. Most of the MotB Cys mutants retained normal swarming ability, but the MotB Y208C mutant had a significantly decreased swarm size, and the MotB R258C mutant completely lost swarming ability. We confirmed that the MotB R258C mutant lost swimming ability in liquid medium by dark-field microscopy and that it possessed normal flagella by electron microscopy (data not shown). The MotB R258C mutation was identified previously after random mutagenesis as causing a dominant, non-functional mutant (*43*). These results suggest that the MotB Tyr^{208} and Arg^{258} residues have important roles in motor function, and that Arg^{258}, in particular, may play a critical role.

We previously performed a Cys modification assay using mPEG-maleimide (*38*). The thiol-specific reagent mPEG-maleimide is a very large molecule whose molecular mass is about 5,000 Da, so we are able to evaluate Cys modification by mobility shifts of the bands on SDS–PAGE gels. By this assay, we speculated which residues of the C-terminal region of the MotB protein are exposed on the surface. We quantified the mPEG-maleimide labeling efficiencies by dividing the intensity of the shifted band by the total band intensity of each MotB Cys mutant (Fig. 1D). MotB D198C, S248C and A278C showed high labeling efficiencies; in contrast, MotB A218C, R258C and R308C were not labeled at all.

MotB-Pal Chimeric Protein and its Motile Revertants—*E. coli* Pal is one of the best-studied PGB proteins biochemically and structurally. To clarify the role of the C-terminal PGB region of MotB, we constructed a chimeric *E. coli* MotB protein in which the C-terminal regions was replaced by the PGB region of *E. coli* Pal. The design of the chimeric MotB protein (hereafter refer to as MotB-Pal) is shown in Fig. 2A. We positioned the junction site of chimeric protein just after the slightly variable β-sheet corresponding to the β1 in *H. influenzae* Pal (*19*) in the PGB region. To keep the phenylalanine residue of Pal which is conserved among *E. coli* PGB proteins (*19*), we replaced the MotB C-terminal region with Pal as follows: $Q^{156}NRPM^{160}/F^{52}DLDK^{56}$ (the former half is from *E. coli* MotB, the latter half is from *E. coli* Pal).

We transformed the *E. coli* Δ*motAB* strain RP6894 with a pJN726-based plasmid that expresses the genes encoding *E. coli* MotA and the constructed MotB-Pal chimeric protein under an L-arabinose-inducible promoter (pJFM10). This transformed cells did not show any swarming ability even when incubated for 24 h on soft agar plates (Fig. 2B). When these mutants were observed in liquid medium under dark-field microscopy, we did not observe any swimming cells (data not shown). Next, we carried out immunoblotting using anti-MotB antibodies (Fig. 2C). These antibodies recognize a peptide sequence at the N-terminus of *E. coli* MotB. As a result, we detected about the same amount of MotB-Pal as of wild-type MotB. The levels of plasmid-encoded MotA were also similar in the two strains (data not shown). When the MotB chimera was expressed in wild-type *E. coli* strain RP437, no negative dominant effect on motility was observed (Fig. 2D). Amounts of the wild-type MotB and the MotB chimera protein were not changed even when the both proteins were co-expressed (Fig. 2E).

Next, we attempted to isolate motile revertants of the Δ*motAB* strain producing the MotB-Pal chimeric protein. The cells were streaked on soft agar T-broth plates, and incubated at 30°C for a few days. Several motile mutants were isolated from swarm-restoring flares. The plasmids were obtained from each isolate and were reintroduced into fresh Δ*motAB* cells. We isolated transformants with restored swarming ability again, and identified four independent mutations in the MotB-Pal protein. One was MotB-Pal F172V (TTC to GTC, named sp1) and the other three had the same mutation, MotB-Pal P159L (CCG to CTG, named sp2, 3 and 4); we show only the results obtained with sp1 and sp2. The sites of the mutations in the MotB-Pal motile revertants are indicated in Fig. 2A and F. These two mutations are closely positioned around the chimeric junction site. MotB-Pal F172V was located in the Pal part of the protein; in contrast, P159L was in the MotB portion. These motile revertants did not restore swarming ability to the level of wild-type cells, but they clearly exhibited swarming after 24-h incubation on soft agar plates (Fig. 2B). Protein amounts of these revertants were almost the same as the original MotB-Pal (Fig. 2C) and MotA proteins (data not shown), suggesting that the stability of the revertant proteins was not changed by the mutations. No negative dominant effect on wild-type motility was observed even when the MotB-Pal revertants were expressed in the wild-type strain (Fig. 2D and 2E). This result implies that MotB-Pal can not be assembled with MotA efficiently to form a stator complex or the chimeric stator complexes can not be assembled efficiently compared to the wild-type stator. These implications are consistent with the result that the chimeric stator complexes conferred only small swarming ability.

The Various Amino Acid Mutations and PG-binding Ability of MotB-Pal Motile Revertants—We investigated the effect of side-chain variation at the position of Phe^{172} in MotB-Pal on motility. We performed site-directed mutagenesis to substitute the MotB-Pal Phe^{172} residue with eight other amino acids including Val, which was present in the spontaneous motile revertant. The MotB-Pal F172A mutant conferred the same motility as the F172V mutant (Fig. 3A). In contrast, the F172S, F172C and F172Y mutants supported weak motility that led to spreading of the colonies after two days incubation (data not shown), whereas the F172G, F172L and F172P mutants were completely non- motile. The protein levels for each mutant were almost the same as for the original MotB-Pal except for F172P of which the protein level was remarkably decreased (data not shown). The F172P mutation may cause the structural change and

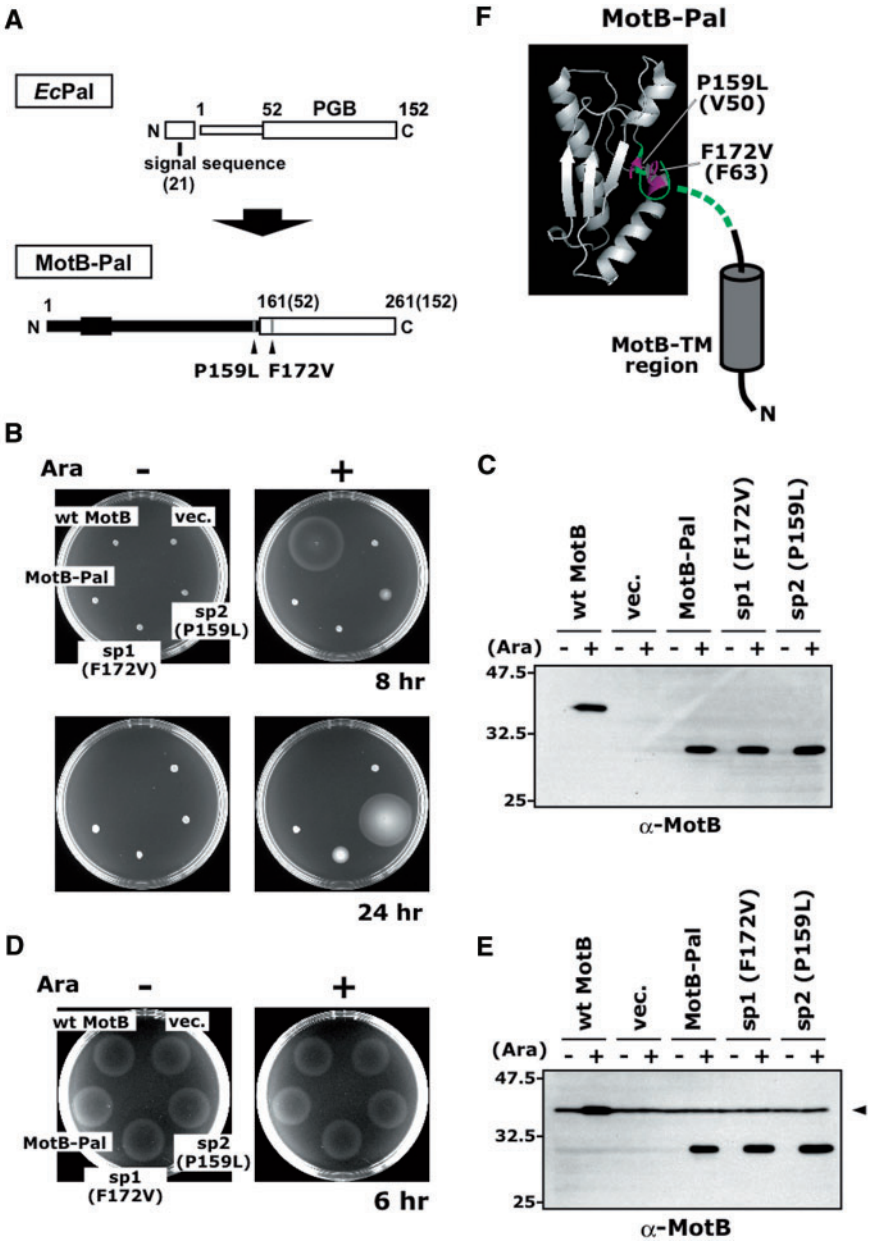

Fig. 2. **Function of the MotB-Pal chimera and its motile revertants.** (A) Diagram of the construction of the MotB-Pal chimera. *Upper*: Primary structure of *E. coli* Pal. The 21-amino-acid signal sequence is cleaved when the pre-mature proteins are transported to the periplasmic space. The Pal protein associates with PG via its C-terminal PGB domains. *Lower*: the chimeric protein constructed in this work. The C-terminal region of *E. coli* MotB was replaced with the PGB region of the Pal. The arrowheads indicate the position of the mutations in the MotB-Pal motile revertants. (B) Motility of the cells expressing MotB-Pal chimera or its motile revertants. Swarm assays for the RP6894 (Δ*motAB*) cells harboring pJN726 (MotA/MotB), pBAD24 (vector), pJFM10 (MotA/MotB-Pal), pJFM10sp1 (MotA/MotB-Pal F172V) or pJFM10sp2 (MotA/MotB-Pal P159L) were performed. A drop (2 μl) of overnight culture was inoculated on 0.27% soft-agar T broth plates in the presence (+) or absence (−) of 0.04% L-arabinose and incubated at 30°C for 8 h (*Upper*) or 24 h (*Lower*). In the condition of 24 h incubation, the Δ*motAB* strain producing MotA/MotB was removed. (C) Products of the MotB-Pal chimera or its revertants expressing cells. In the presence (+) or absence (−) of 0.04% L-arabinose, proteins from RP6894 (Δ*motAB*) cells harboring pJN726, pBAD24, pJFM10, pJFM10sp1 or pJFM10sp2 were detected by immunoblotting using anti-MotB antibodies. Estimated sizes are 34 kDa (wt MotB) and 29 kDa (MotB-Pal and its revertants). (D and E) Co-expression of MotB-Pal chimera or its revertants with wild-type MotB. Swarm assay (D) and immunoblot (E) were performed as the same condition with (B) and (C), respectively, except the host strain which was RP437 (wild-type). The arrowhead on the right side in (E) indicates the intrinsic wild-type MotB derived from the chromosome. (F) Schematic diagram of the motile revertants of MotB-Pal expressing strains. Predicted structure of MotB-Pal is shown. Ribbon presentation is the structure of *E. coli* Pal (PDB accession code 1oap) visualized using PyMOL (http://pymol.sourceforge.net/). The MotB region is shown in the drawing (TM region) and green color (switching region). Position of the MotB-Pal Phe^{172} (Phe^{63} in *E. coli* Pal) and predicted position of Pro^{159} [Val^{50} in *E. coli* Pal, predicted from the sequence alignment reported in Kojima *et al*. (*21*)] are shown in magenta.

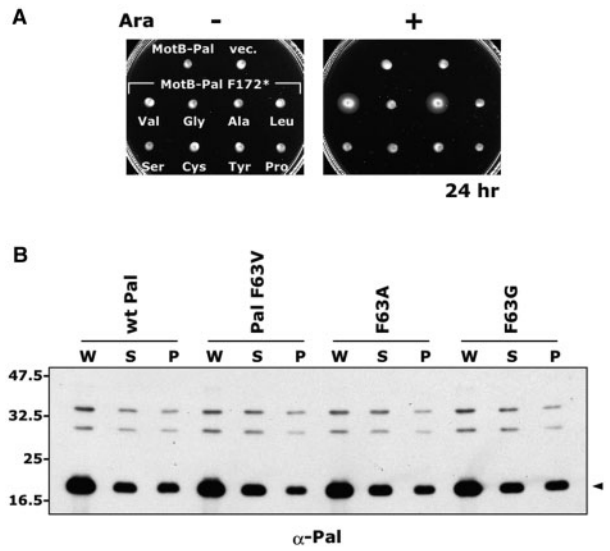

Fig. 3. **Evaluation of peptidoglycan-binding of the MotB-Pal Phe^{172} mutants.** (A) Site-directed mutagenesis of the MotB-Pal Phe^{172} residue. Swarm assays for the RP6894 (Δ*motAB*) cells harboring pJFM10 (MotA/MotB-Pal), pBAD24 (vector) or MotB-Pal Phe^{172} variants substituted with eight amino acids. A drop (2 μl) of overnight culture was inoculated on 0.27% soft-agar T broth plates in the presence (+) or absence (−) of 0.04% L-arabinose and incubated at 30°C for 24 h. (B) PG-binding assay of the *E. coli* Pal Phe^{63} mutants. PG-binding Pal proteins were analyzed in the JC7752 (Δ*tolB-pal*) cells harboring pYZ501 (wt Pal) or its derivatives Pal F63V, F63A or F63G. Substitutions corresponding to F63V and F63A in the MotB-Pal protein restored motility, while F63G did not restore motility. Cells were solubilized with 2% SDS and PG-binding proteins were collected by ultracentrifugation as insoluble pellets. W, whole cell; S, soluble (supernatant) fraction; P, insoluble (pellet) fraction. Each fraction was analysed by SDS–PAGE and immunoblotting using anti-*Ec* Pal antibodies. The arrowhead at the right shows the Pal protein.

reduce the protein stability. We could not find clear rules determining which side-chains at position 172 restored MotB function, but the evidence that Ala, Val, Ser or Cys substitutions restored function and Gly or Leu did not restore motility might suggest that side-chains that were too short or too long were not suitable to restore function, although a Tyr substitution could not be applied. These results gave us some amino acid candidates to introduce into the Pal protein to assess the PG-binding ability of the MotB-Pal.

In a recent study, the PG-binding abilities of the *Salmonella* MotB and a transmembrane-truncated MotB fragment were assayed (*44*). It has been shown that neither MotB nor its C-terminal fragment is detected in the PG-binding fraction, although the Pal protein shows strong binding to PG. This result implies that the manner of PG-binding of MotB is different from that of Pal, *e.g.* MotB-binding to PG may be weaker than Pal or may be inactivated when MotB is not incorporated into the motor (*44*). This idea raises the possibility that the restoration of motility of the MotB-Pal revertant was caused by changes in the PG-binding ability. To investigate this possibility, we analysed PG-binding of the MotB-Pal and its revertant by using the method described by Cascales and Llobes (*33*) to detect PG-binding of Pal. Briefly, cells were solubilized with 2% SDS and PG-binding proteins were collected by ultracentrifugation as insoluble pellets. We initially performed PG-binding assays for MotB, MotB-Pal and its revertant, but we did not detect any associated proteins in the PG-binding fraction (data not shown).

We introduced three residue substitutions at the Phe^{63} residue of Pal, which corresponds to Phe^{172} of MotB-Pal. The Val and Ala substitutions restored the motility function of MotB-Pal, whereas the Gly substitution did not (Fig. 3A). We transformed the *E. coli* Δ*tolB-pal* strain JC7752 with plasmid pYZ501 or its derivatives expressing the *E. coli* Pal protein or Pal F63V, F63A or F63G mutant proteins. We performed PG-binding assays on these constructed strains. The resulting levels of wild-type Pal protein and its derivatives in the PG-binding fractions turned out to be almost the same (Fig. 3B, compare each lane 'P'). This result indicates that the substitution of the Phe^{63} residue in Pal does not affect its ability to bind to PG, although the same change in MotB-Pal alters its MotB function.

DISCUSSION

The PGB Region of MotB is Exchangeable with the PGB Region of Pal—MotB has a PGB region and is the flagellar motor component that forms the stator complex with MotA to generate the driving force for rotation. It is believed that the stator is anchored by the PGB region. Pal also has a PGB region and is a component of the Tol-Pal system, which maintains cell envelope integrity. In this work, we have shown that the chimeric MotB protein, in which the C-terminal PGB region of MotB has been replaced with the Pal PGB region, acquires MotB function with single amino-acid substitutions (Fig. 2B). A substitution at Phe^{172} of MotB-Pal that restored motility did not change binding to PG when they were replaced the corresponding Phe^{63} residue of Pal (Fig. 3B). This implies that the MotB-Pal motile revertants acquired MotB function without affecting PG-binding. The MotB-Pal chimera as well as its revertants showed no dominant negative effect on wild-type motility (Fig. 2D). We speculate that MotB-Pal has poor or no ability to form a stator complex with MotA or the MotA/MotB-Pal stator complex has poor or no ability to assemble around the rotor.

Why were the MotB-Pal revertants able to function as MotB? It has been reported that one of these mutation sites, Pro^{159}, gave a dominant-negative phenotype for the intact *E. coli* MotB (*43*). This mutant, MotB P159I, was partially functional and many motile suppressors were isolated. Suppressor mutations were found in MotA and in the motor switch components, FliG and FliM (*45*, *46*). The authors' interpretation of these results was that the MotB P159I mutation distorts a correct spatial relationship between the stator and the rotor that is essential for torque generation but the suppressor mutations in MotA or the switch complex proteins caused realignment of these components. Therefore, the MotB Pro^{159} residue seems to be an important residue that affects the arrangement of MotA/MotB stator complex relative to

the switch complex. It is an another speculation for the MotB-Pal motile revertants that the MotB-Pal chimera disrupted positioning of the stator complex and the additional P159L mutation resulted in realignment of the stator, restored correct motor-stator interaction and acquired motor function. The other revertant, MotB-Pal F172V, has a mutation near the Pro^{159} residue based on the predicted structure (Fig. 2F), suggesting that a similar structural change as that caused by P159L was generated by the Phe^{172} mutations although the motility was not as good as that of the P159L revertant.

Mapping of the MotB Cys Variants on the Structure of the Pal PGB Region—Pal is one of the best-characterized PGB proteins and the recognition of and binding to PG has been well studied. Moreover, the crystal structure of *E. coli* Pal (PDB accession code 1oap) and the NMR structure of *H. influenzae* Pal with a biosynthetic PG-precursor (*19*) have been reported. In this study, we show that the PGB region of the MotB C-terminus can be exchanged with that of *E. coli* Pal at least with respect to PG-binding. If the mechanism for PG-association of the PGB region of MotB and Pal is the same, the structures of their PGB regions would also be expected to be similar to each other. This assumption is supported by a crystal structure of the C-terminal periplasmic domain of MotB (*18*). To evaluate structural similarities between *E. coli* MotB and *E. coli* Pal and to obtain new insights about the PGB region of MotB on the basis of the mechanism for PG-association of Pal, we mapped the substituted residues in the MotB Cys-mutagenesis experiment on the crystal structure of the *E. coli* Pal protein (Fig. 4). Residues corresponding to each mutation site were determined by secondary structure prediction and sequence alignment of the various PGB proteins (*21*). Because MotB turned out to possess about 40 extra amino acids (Asn^{266} to Arg^{308}) in its C-terminus compared to Pal, we could not map the last five mutation sites on the Pal structure (MotB Q268C, A278C, L288C, S298C and R308C). But this region is dispensable for MotB function, because deletion and truncation analyses of MotB indicated that a 39-amino-acid deletion of the C-terminus had little effect on motility and protein stability (*47*, *48*).

In the Cys modification experiment, using mPEG-maleimide (Fig. 1D), MotB D198C and S248C showed high labeling efficiencies. In the Pal map (Fig. 4A), D198 (orange) and S248 (red) were located close together and formed a protrusion from the 'top' of the structure. Their surface-exposure on this protrusion may explain the high labeling efficiency by mPEG-maleimide, suggesting that this mapping provides a reasonable model of the MotB C-terminus. It is noteworthy that both loop regions on which these two residues were positioned are disordered in the corresponding region of the crystal structure of the *V. alginolyticus* MotY, which is a flagellar T-ring component and also a PG-binding protein (*21*). As proposed in that report, the loop region of MotY may regulate the binding affinity to PG to prevent tight binding to the PG layer before it associates with the flagellar-basal body. MotB must avoid being strongly bound to the PG layer before it assembles and functions around the flagellar-basal body. Our data from the Cys-modification experiment demonstrate that this loop region of

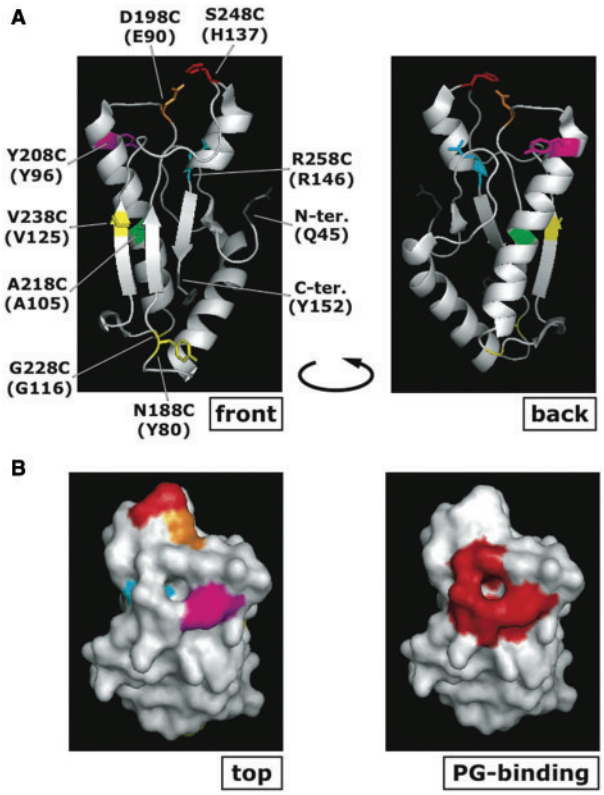

Fig. 4. **Mapping of the MotB Cys variants on the Pal structure.** (A) Ribbon structures of *E. coli* Pal (1oap) visualized using PyMOL (http://pymol.sourceforge.net/) are presented. Predicted positions of the MotB Cys variants studied in this work except the MotB-specific region (MotB Q268C, A278C, L288C, S298C and R308C) were mapped on the Pal structure. Each position was predicted by secondary structure prediction and sequence alignment of various PGB proteins (*21*). Colour codes and characteristics of each MotB Cys variant are as follows. MotB D198C (orange) and S248C (red) were efficiently modified by mPEG-maleimide; in contrast, A218C (green) and R258C (cyan) were not modified. MotB Y208C (magenta) caused reduced motility; furthermore, R258C resulted in a completely non-motile phenotype. MotB N188C, G228C and V238C are shown in yellow. The N- and C-termini of this Pal structure are shown in gray. Residue numbers in parentheses indicate *E. coli* Pal numbering. (B) Comparison with predicted PG-binding residues. *Left*: Top view of the surface model of the right panel in (A). *Right*: the predicted residues contributing to PG-binding (MotB Phe^{161} (Pal Phe^{52}), Thr^{163} (Leu^{54}), Gly^{164} (Asp^{55}), Asp^{197} (Asp^{89}), Phe^{199} (Arg^{91}), Ser^{209} (Tyr^{96}), Leu^{213} (Leu^{100}) and Arg^{217} (Arg^{104}), proposed by Kojima *et al*. (*21*) are shown in red.

MotB is highly accessible to solvent. Thus, this loop region of MotB may also regulate the binding affinity to PG in a similar manner as in MotY. In contrast to the residues mentioned above, MotB A218C and MotB R258C showed no labeling by mPEG-maleimide. In the Pal map (Fig. 4A), A218 (green) was buried in the core, and R258 (cyan) was also positioned inside, although the side chain of the Arg residue was predicted to be slightly surface-exposed. The side chain of the Arg residue is fairly long compared to other amino acids, so it is possible for this residue to be buried in the core when substituted with a Cys residue with a short side chain.

In the motility assays (Fig. 1C), the MotB Y208C (magenta) mutation caused partially defective motility, and R258C (cyan) completely lost motility. In the Pal map (Fig. 4A), these two residues are located near the upper part of the loop region on one side (back) of the structure. Based on the structure of the *H. influenzae* Pal with the PG-precursor, the residues contributing to binding to PG in the structure of the Pal-PGB region have been predicted (*19*, *21*). Interestingly, these predicted PG-binding residues in Pal (Fig. 4B, right panel) overlapped with or were located very close to the corresponding mutated residues in MotB that severely affected motility (Fig. 4B, left panel). Moreover, the *E. coli* Pal R146H mutant, of which mutation site is corresponding to Arg^{258} of *E. coli* MotB, has been reported to have lost the ability to associate with PG (*49*). So far, direct binding of MotB to PG has not been shown; however, our data suggest that MotB binds directly to PG via its PGB region in a similar manner to that of Pal.

Recently, a crystal structure of the C-terminal PGB region of MotB from *H. pylori* was solved (*18*). As expected, its protein fold was very similar to that of *E. coli* Pal and other PGB proteins. We tried to map the *E. coli* MotB Cys mutants on this structure, and obtained almost the same results as with *E. coli* Pal. This supports the assumption that *E. coli* MotB and *E. coli* Pal have the structural and functional similarity and are exchangeable. Interestingly, the sequence homology between the C-terminal PGB region of *E. coli* MotB (a.a. 161–308) and *H. pylori* MotB (a.a. 125–256) was lower than that between *E. coli* MotB and *E. coli* Pal (a.a. 52–152); 20% identity versus 24% identity. We assume that the structure for the PG association would be more conserved among PGB proteins in the same species than proteins with the same function of different species in which the PG structures are possible to differ.

Functional Comparison with the Tol-Pal System and Dynamic Movement of the Stator—In the Tol-Pal system, which is structurally homologous with the Mot system in the flagellar motor, extensive studies have been carried out to elucidate the proton motive force (pmf)-dependent change in conformation and interaction of the components in the system. It has been found that the interaction between Pal and the C-terminal periplasmic domain of the transmembrane protein TolA and the conformational change in TolA are dependent on pmf (*50*, *51*). This pmf-dependent change in the periplasmic domain of TolA has been reported to be energized by the two transmembrane proteins, TolQ and TolR, which form a putative ion channel (*34*, *35*). Cysteine scanning experiments on the C-terminal domain of the TolR, which has a large C-terminal periplasmic domain and a predicted role in regulating ion flow, revealed that pmf also causes a conformational change in the TolR periplasmic domain (*52*). Recently, the NMR structure of the C-terminal periplasmic domain of the *H. influenzae* TolR has been reported, and this 3D structure is very similar to the conventional PGB domain of other proteins (*53*). From the evidence of the Tol-Pal system and the structural and functional similarities revealed by our MotB-Pal chimera experiments, it is easy to imagine that the conformation of the MotA/MotB stator complex, especially the periplasmic PGB region of MotB, is also changed by pmf. The MotA/MotB stator complex should be anchored around the rotor only when assembled into the motor, so these conformational changes might reflect dynamic movement of the stator as reported by fluorescence studies (*54*, *55*). To elucidate the mechanism of dynamic assembly and conformational change of the stator, the interaction between the stator and the basal body is an important topic that should be addressed. It is widely believed that the cytoplasmic domain of MotA in the stator interacts with the C-terminal region of FliG, a C-ring component of the rotor. On the other hand, in the periplasmic space the P ring, which is located in the PG layer, may interact with the periplasmic domain of MotB in the stator, although this idea is very speculative. In the future, we plan to evaluate the possible interaction between the C-terminal PGB domain of MotB and the P ring. This should lead to a new understanding of the ion-flux-driven dynamic movement of the stator complex.

ACKNOWLEDGEMENTS

We thank Ikuro Kawagishi for assisting the design of this study and invaluable suggestions, and Yuki Sudo and Kingo Takiguchi for helpful discussions. We acknowledge Hélène Bénédetti and Shin-ichiro Narita for the gift of the strain JC7752, and Hajime Tokuda for the anti-*E. coli* Pal antibodies. J.F.M., who was an undergraduate student at the University of Manchester, was supported by the exchange program between the two universities and by the Nagoya University Program for Academic Exchange (NUPACE).

FUNDING

Scientific research from the Japan Society for the Promotion of Science (to Y.H., M.H. and S.K.) in part; from the Ministry of Education, Culture, Sports, Science and Technology of Japan (to M.H and S.K.).

CONFLICT OF INTEREST

None declared.

REFERENCES

1. Macnab, R.M. (2003) How bacteria assemble flagella. *Annu. Rev. Microbiol.* **57**, 77–100
2. Blair, D.F. (2003) Flagellar movement driven by proton translocation. *FEBS Lett.* **545**, 86–95
3. Francis, N.R., Sosinsky, G.E., Thomas, D., and DeRosier, D.J. (1994) Isolation, characterization and structure of bacterial flagellar motors containing the switch complex. *J. Mol. Biol.* **235**, 1261–1270
4. Dean, G.E., Macnab, R.M., Stader, J., Matsumura, P., and Burks, C. (1984) Gene sequence and predicted amino acid sequence of the *motA* protein, a membrane-associated protein required for flagellar rotation in *Escherichia coli*. *J. Bacteriol.* **159**, 991–999
5. Stader, J., Matsumura, P., Vacante, D., Dean, G.E., and Macnab, R.M. (1986) Nucleotide sequence of the *Escherichia coli motB* gene and site-limited incorporation of its product into the cytoplasmic membrane. *J. Bacteriol.* **166**, 244–252

6. Blair, D.F. and Berg, H.C. (1990) The MotA protein of *E. coli* is a proton-conducting component of the flagellar motor. *Cell* **60**, 439–449
7. Stolz, B. and Berg, H.C. (1991) Evidence for interactions between MotA and MotB, torque-generating elements of the flagellar motor of *Escherichia coli*. *J. Bacteriol.* **173**, 7033–7037
8. Zhou, J., Fazzio, R.T., and Blair, D.F. (1995) Membrane topology of the MotA protein of *Escherichia coli*. *J. Mol. Biol.* **251**, 237–242
9. Chun, S.Y. and Parkinson, J.S. (1988) Bacterial motility: membrane topology of the *Escherichia coli* MotB protein. *Science* **239**, 276–278
10. De Mot, R. and Vanderleyden, J. (1994) The C-terminal sequence conservation between OmpA-related outer membrane proteins and MotB suggests a common function in both gram-positive and gram-negative bacteria, possibly in the interaction of these domains with peptidoglycan. *Mol. Microbiol.* **12**, 333–334
11. Sato, K. and Homma, M. (2000) Functional reconstitution of the Na^+-driven polar flagellar motor component of *Vibrio alginolyticus*. *J. Biol. Chem.* **275**, 5718–5722
12. Yorimitsu, T., Kojima, M., Yakushi, T., and Homma, M. (2004) Multimeric structure of the PomA/PomB channel complex in the Na^+-driven flagellar motor of *Vibrio alginolyticus*. *J. Biochem.* **135**, 43–51
13. Kojima, S. and Blair, D.F. (2004) Solubilization and purification of the MotA/MotB complex of *Escherichia coli*. *Biochemistry* **43**, 26–34
14. Braun, T.F., Al-Mawsawi, L.Q., Kojima, S., and Blair, D.F. (2004) Arrangement of core membrane segments in the MotA/MotB proton-channel complex of *Escherichia coli*. *Biochemistry* **43**, 35–45
15. Zhou, J., Sharp, L.L., Tang, H.L., Lloyd, S.A., Billings, S., Braun, T.F., and Blair, D.F. (1998) Function of protonatable residues in the flagellar motor of *Escherichia coli*: a critical role for Asp^{32} of MotB. *J. Bacteriol.* **180**, 2729–2735
16. Kojima, S. and Blair, D.F. (2001) Conformational change in the stator of the bacterial flagellar motor. *Biochemistry* **40**, 13041–13050
17. Koebnik, R. (1995) Proposal for a peptidoglycan-associating alpha-helical motif in the C-terminal regions of some bacterial cell-surface proteins. *Mol. Microbiol.* **16**, 1269–1270
18. Roujeinikova, A. (2008) Crystal structure of the cell wall anchor domain of MotB, a stator component of the bacterial flagellar motor: implications for peptidoglycan recognition. *Proc. Natl Acad. Sci. USA* **105**, 10348–10353
19. Parsons, L.M., Lin, F., and Orban, J. (2006) Peptidoglycan recognition by Pal, an outer membrane lipoprotein. *Biochemistry* **45**, 2122–2128
20. Grizot, S. and Buchanan, S.K. (2004) Structure of the OmpA-like domain of RmpM from *Neisseria meningitidis*. *Mol. Microbiol.* **51**, 1027–1037
21. Kojima, S., Shinohara, A., Terashima, H., Yakushi, T., Sakuma, M., Homma, M., Namba, K., and Imada, K. (2008) Insights into the stator assembly of the *Vibrio* flagellar motor from the crystal structure of MotY. *Proc. Natl Acad. Sci. USA* **105**, 7696–7701
22. Matsuyama, S., Tajima, T., and Tokuda, H. (1995) A novel periplasmic carrier protein involved in the sorting and transport of *Escherichia coli* lipoproteins destined for the outer membrane. *EMBO J.* **14**, 3365–3372
23. Matsuyama, S., Yokota, N., and Tokuda, H. (1997) A novel outer membrane lipoprotein, LolB (HemM), involved in the LolA (p20)-dependent localization of lipoproteins to the outer membrane of *Escherichia coli*. *EMBO J.* **16**, 6947–6955
24. Yokota, N., Kuroda, T., Matsuyama, S., and Tokuda, H. (1999) Characterization of the LolA-LolB system as the general lipoprotein localization mechanism of *Escherichia coli*. *J. Biol. Chem.* **274**, 30995–30999
25. Yakushi, T., Masuda, K., Narita, S., Matsuyama, S., and Tokuda, H. (2000) A new ABC transporter mediating the detachment of lipid-modified proteins from membranes. *Nat. Cell. Biol.* **2**, 212–218
26. Mizuno, T. (1979) A novel peptidoglycan-associated lipoprotein found in the cell envelope of *Pseudomonas aeruginosa* and *Escherichia coli*. *J. Biochem.* **86**, 991–1000
27. Lazzaroni, J.C. and Portalier, R. (1992) The *excC* gene of *Escherichia coli* K-12 required for cell envelope integrity encodes the peptidoglycan-associated lipoprotein (PAL). *Mol. Microbiol.* **6**, 735–742
28. Leduc, M., Ishidate, K., Shakibai, N., and Rothfield, L. (1992) Interactions of *Escherichia coli* membrane lipoproteins with the murein sacculus. *J. Bacteriol.* **174**, 7982–7988
29. Bouveret, E., Benedetti, H., Rigal, A., Loret, E., and Lazdunski, C. (1999) In vitro characterization of peptidoglycan-associated lipoprotein (PAL)-peptidoglycan and PAL-TolB interactions. *J. Bacteriol.* **181**, 6306–6311
30. Lloubes, R., Cascales, E., Walburger, A., Bouveret, E., Lazdunski, C., Bernadac, A., and Journet, L. (2001) The Tol-Pal proteins of the *Escherichia coli* cell envelope: an energized system required for outer membrane integrity? *Res. Microbiol.* **152**, 523–529
31. Walburger, A., Lazdunski, C., and Corda, Y. (2002) The Tol/Pal system function requires an interaction between the C-terminal domain of TolA and the N-terminal domain of TolB. *Mol. Microbiol.* **44**, 695–708
32. Ray, M.C., Germon, P., Vianney, A., Portalier, R., and Lazzaroni, J.C. (2000) Identification by genetic suppression of *Escherichia coli* TolB residues important for TolB-Pal interaction. *J. Bacteriol.* **182**, 821–824
33. Cascales, E. and Lloubes, R. (2004) Deletion analyses of the peptidoglycan-associated lipoprotein Pal reveals three independent binding sequences including a TolA box. *Mol. Microbiol.* **51**, 873–885
34. Cascales, E., Lloubes, R., and Sturgis, J.N. (2001) The TolQ-TolR proteins energize TolA and share homologies with the flagellar motor proteins MotA-MotB. *Mol. Microbiol.* **42**, 795–807
35. Goemaere, E.L., Cascales, E., and Lloubes, R. (2007) Mutational analyses define helix organization and key residues of a bacterial membrane energy-transducing complex. *J. Mol. Biol.* **366**, 1424–1436
36. Eick-Helmerich, K. and Braun, V. (1989) Import of biopolymers into *Escherichia coli*: nucleotide sequences of the *exbB* and *exbD* genes are homologous to those of the *tolQ* and *tolR* genes, respectively. *J. Bacteriol.* **171**, 5117–5126
37. Sambrook, J., Fritsch, E.F., and Maniatis, T. (1989) *Molecular Cloning: A Laboratory Manual*, 2nd edn. Cold Spring Harbor Laboratory, Cold Spring Harbor, NY
38. Hizukuri, Y., Kojima, S., Yakushi, T., Kawagishi, I., and Homma, M. (2008) Systematic Cys mutagenesis of FlgI, the flagellar P-ring component of *Escherichia coli*. *Microbiology* **154**, 810–817
39. Irieda, H., Homma, M., Homma, M., and Kawagishi, I. (2006) Control of chemotactic signal gain via modulation of a pre-formed receptor array. *J. Biol. Chem.* **281**, 23880–23886
40. Yakushi, T., Hattori, N., and Homma, M. (2005) Deletion analysis of the carboxyl-terminal region of the PomB component of the *Vibrio alginolyticus* polar flagellar motor. *J. Bacteriol.* **187**, 778–784
41. Fukuoka, H., Yakushi, T., Kusumoto, A., and Homma, M. (2005) Assembly of motor proteins, PomA and PomB, in the Na^+-driven stator of the flagellar motor. *J. Mol. Biol.* **351**, 707–717
42. Braun, T.F. and Blair, D.F. (2001) Targeted disulfide cross-linking of the MotB protein of *Escherichia coli*: evidence for two H^+ channels in the stator complex. *Biochemistry* **40**, 13051–13059

43. Blair, D.F., Kim, D.Y., and Berg, H.C. (1991) Mutant MotB proteins in *Escherichia coli*. *J. Bacteriol.* **173**, 4049–4055
44. Kojima, S., Furukawa, Y., Matsunami, H., Minamino, T., and Namba, K. (2008) Characterization of the periplasmic domain of MotB and implications for its role in the stator assembly of the bacterial flagellar motor. *J. Bacteriol.* **190**, 3314–3322
45. Garza, A.G., Harris-Haller, L.W., Stoebner, R.A., and Manson, M.D. (1995) Motility protein interactions in the bacterial flagellar motor. *Proc. Natl Acad. Sci. USA* **92**, 1970–1974
46. Garza, A.G., Biran, R., Wohlschlegel, J.A., and Manson, M.D. (1996) Mutations in *motB* suppressible by changes in stator or rotor components of the bacterial flagellar motor. *J. Mol. Biol.* **258**, 270–285
47. Muramoto, K. and Macnab, R.M. (1998) Deletion analysis of MotA and MotB, components of the force-generating unit in the flagellar motor of *Salmonella*. *Mol. Microbiol.* **29**, 1191–1202
48. Van Way, S.M., Hosking, E.R., Braun, T.F., and Manson, M.D. (2000) Mot protein assembly into the bacterial flagellum: a model based on mutational analysis of the *motB* gene. *J. Mol. Biol.* **297**, 7–24
49. Clavel, T., Germon, P., Vianney, A., Portalier, R., and Lazzaroni, J.C. (1998) TolB protein of *Escherichia coli* K-12 interacts with the outer membrane peptidoglycan-associated proteins Pal, Lpp and OmpA. *Mol. Microbiol.* **29**, 359–367
50. Germon, P., Ray, M.C., Vianney, A., and Lazzaroni, J.C. (2001) Energy-dependent conformational change in the TolA protein of *Escherichia coli* involves its N-terminal domain, TolQ, and TolR. *J. Bacteriol.* **183**, 4110–4114
51. Cascales, E., Gavioli, M., Sturgis, J.N., and Lloubes, R. (2000) Proton motive force drives the interaction of the inner membrane TolA and outer membrane Pal proteins in *Escherichia coli*. *Mol. Microbiol.* **38**, 904–915
52. Goemaere, E.L., Devert, A., Lloubes, R., and Cascales, E. (2007) Movements of the TolR C-terminal domain depend on TolQR ionizable key residues and regulate activity of the Tol complex. *J. Biol. Chem.* **282**, 17749–17757
53. Parsons, L.M., Grishaev, A., and Bax, A. (2008) The periplasmic domain of TolR from *Haemophilus influenzae* forms a dimer with a large hydrophobic groove: NMR solution structure and comparison to SAXS data. *Biochemistry* **47**, 3131–3142
54. Leake, M.C., Chandler, J.H., Wadhams, G.H., Bai, F., Berry, R.M., and Armitage, J.P. (2006) Stoichiometry and turnover in single, functioning membrane protein complexes. *Nature* **443**, 355–358
55. Fukuoka, H., Wada, T., Kojima, S, Ishijima, A., and Homma, M. (2009) Sodium-dependent dynamic assembly of membrane complexes in sodium-driven flagellar motors. *Mol. Microbiol.* **71**, 825–835
56. Parkinson, J.S. and Houts, S.E. (1982) Isolation and behavior of *Escherichia coli* deletion mutants lacking chemotaxis functions. *J. Bacteriol.* **151**, 106–113
57. Bouveret, E., Derouiche, R., Rigal, A., Lloubes, R., Lazdunski, C., and Benedetti, H. (1995) Peptidoglycan-associated lipoprotein-TolB interaction. A possible key to explaining the formation of contact sites between the inner and outer membranes of *Escherichia coli*. *J. Biol. Chem.* **270**, 11071–11077
58. Guzman, L.M., Belin, D., Carson, M.J., and Beckwith, J. (1995) Tight regulation, modulation, and high-level expression by vectors containing the arabinose P_{BAD} promoter. *J. Bacteriol.* **177**, 4121–4130